Phys. Status Solidi C **7**, No. 2, 153–156 (2010) / **DOI** 10.1002/pssc.200982459

physica status solidi c
www.pss-c.com
*current topics in solid state physics*

# The physics of highly ordered molecular rows

**S. Blankenburg**[*], **E. Rauls, and W. G. Schmidt**

Lehrstuhl für Theoretische Physik, Universität Paderborn, 33095 Paderborn, Germany

Received 5 July 2009, revised 6 October 2009, accepted 14 October 2009
Published online 3 December 2009

**PACS** 31.15.A-, 68.43.-h, 73.20.-r, 82.45.Jn

[*] Corresponding author: blank@phys.upb.de

First-principles calculations are used to rationalize the formation of well-separated molecular rows of glutamic acid on Ag(110) and DEB on Au(111) upon adsorption. The different mechanisms for the row separation are analyzed in detail. The analysis of the energetics underlines the importance of long-range dispersive interactions, which we find crucial to reproduce the experimental results for both systems.



The autonomous ordering and assembly of atoms and molecules on atomically well-defined surfaces appears to be a very promising alternative route to even smaller functional systems with nanometer dimensions [1,2]. However, the mechanisms controlling the self-ordering phenomena need to be thoroughly understood in order to employ self-assembly and growth processes and create taylor-made surface nanostructures. The detailed analysis of prototypical, well-defined model systems from first-principles calculations is an useful first step [3–10].

In the particular context of noncovalent synthesis, the application of amino acids and rosette molecules results in highly ordered and useful structures [2,11,12]. In this article, we present first principles density functional theory (DFT) calculations on the adsorption of (s)-glutamic acid (Fig. 2) on a Ag(110) and diethylbarbituric (DEB, Fig. 2) acid on a Au(111) surface. Both systems form highly ordered rows assembled upon adsorption. Here, we want to rationalize the mechanisms for the specific row separation.

We have performed DFT calculations using the Vienna Ab Initio Simulation Package (VASP) [13] of DFT and the PW91 functional [14] to model the electron exchange and correlation within the generalized gradient approximation (GGA). The electron-ion interaction is described by the projector-augmented wave (PAW) method [15], which allows for an accurate treatment of the first-row elements as well as the Ag $4d$ and Au $5d$ electrons with a relatively moderate energy cutoff of 340 eV. The surface Brillouin zone is sampled using a $2\times2\times1$ mesh for the glutamic acid system and is restricted to the $\Gamma$ point for the DEB system. While the glutamic adsystem is modeled by periodically repeated slabs, containing six atomic Ag layers plus the adsorbed molecules and a vacuum region equivalent in thickness to about 14 atomic Ag layers, the DEB system just contains two atomic Au layers, the adsorbed DEB molecules and a vacuum region of 15 Å. In the case of molecules weakly bonded to each other or to the surface, dispersion interaction – not accounted for in the GGA – may contribute a sizable percentage of the total interaction energy [16]. In order to assess the influence of these van der Waals (vdW) interaction on the adsorption energetics, we have extended our description by a semiempirical approach based on the London dispersion formula to include the dispersion interaction [17]. This approach has proven to be successful in the description of similar systems [18, 19].

As found by scanning tunneling microscopy (STM) [20], glutamic acid adsorbs on Ag(110) in a variety of ordered overlayer structures in dependence of the adsorption temperature and adlayer coverage. The $(4\times8)$ phase is particularly intriguing, since it is formed by highly ordered molecular chains running along the $[\bar{1}10]$-direction, separated by about 33 Å.

We start by determining the structure of the molecular rows within the $(4\times8)$ translational symmetry and assuming the adsorption of the deprotonated species as observed experimentally [20]. A large number of structural candidates for various coverages were probed. The ener-

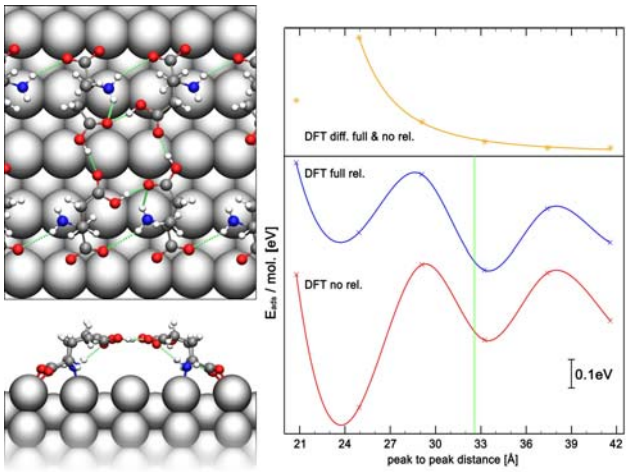


**Figure 1** (color online) Left: Adsorption structures of glutamic acid adsorbed at Ag(110). Hydrogen bonds are indicated with green lines. Right: Adsorption energy per molecule in dependence of the peak to peak distance with and without relaxing the structure as well as the difference between the two curves. Here, a fit with $E \sim A/x^3$ is visualized. The experimental determined distance is marked in green [20].

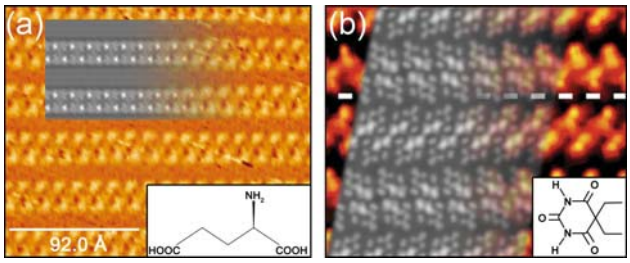


**Figure 2** (color online) Comparison of the calculated and experimental STM images [20, 12] of the (a) (4×8) phase of glutamic acid adsorbed on Ag(110) surface and the (b) DEB molecule at Au(111). The insets represent the schematic molecular structures.

getically most favored model within DFT+vdW is shown in Fig. 1. Here, the short molecule-molecule distances allow multiple hydrogen bonding. The adsorption energy per molecule, $E_{ads} = (E_{tot} - nE_{glu} - E_{subs} + 0.5nE_{H_2})/n$ with $E_{tot}$, $E_{subs}$, $E_{glu}$ and $E_{H_2}$ refering to the energies of the total system, the silver substrate, the adsorbate (s)-glutamic acid, and hydrogen in gas phase, respectively, amount to -1.91 eV.

In Fig. 2 STM images simulated according to the Tersoff-Hamann approach [21] for a bias of -0.67 V are compared with the micrograph measured at the same voltage. Given the methodological problems [22] in simulating the complex (and partially unknown, e.g., tip geometry) physics in modeling STM data, the calculated image stand in a good agreement with the experiment. The measured vibrational frequencies of the adsorbate [20] allow another comparison with the simulation. We calculated the vibrational modes using the frozen phonon approximation [23]. Justified by the significant mass difference between adsorbate and substrate atoms and the corresponding effective decoupling of the respective vibrations, we only include the uppermost two substrate layers in the phonon calculations. A comparison of measured and calculated frequencies is shown in Table 1. As can be seen, the model accounts well for the data assigned to the scissoring mode $\delta_{siss}(NH_2)$, the symmetric stretch mode $v_{sym}(OCO^-)$ and the $v(C{=}O)^{acid}$ mode. Compared to the respective gas-phase vibrations, all modes shift down upon adsorption due to the inter-molecular bonding.

**Table 1** Calculated vibrational modes compared to the experiment. Gas-phase frequencies of the nonzwitterionic molecule are also listed. All values in $cm^{-1}$.

| assignment | exp. [20] | present model | gas-phase |
|---|---|---|---|
| $v(C{=}O)^{acid}$ | 1704 | 1710, 1699 | 1756, 1759 |
| | 1664 | 1675, 1659 | - |
| $\delta_{siss}(NH_2)$ | 1577 | 1565 | 1576 |
| $v_{sym}(OCO^-)$ | 1384 | 1364 | - |

Now the question about the origin of the large and reproducible inter-row distance found experimentally emerges. In principle, two mechanisms could conceivably cause the large spacing between the glutamic-acid rows of the (4×8) phase of the glutamic acid adsorbed Ag(110) surface, substrate-mediated interactions via long-range strain fields [24] or adsorption-induced Friedel oscillations of the electron density at the metal surface [25–27, 8]. By performing calculations where the substrate atoms are either frozen at ideal bulk positions or fully relaxed according to the adsorption induced forces, one can assess the magnitude of strain and charge-density related spatial modulations of the adsorption energy. At first, we neglected strain effects and vary the distance between the molecular rows without taking structural relaxations into account. To this end total energy calculations were performed within a $(4 \times n)$ surface periodicity where $n = 5...10$. The corresponding adsorption energies are shown in Fig. 1. They show a damped oscillation behavior. The wave length and the magnitude of these oscillations is similar to the results obtained in recent calculations for Cu(110) adsorbed adenine and phenylglycine molecules [8]. In this case the modulation of the adsorption energies was explicitly shown to be Friedel-oscillation related. Here the situation is more complex. While the experimentally determined inter-row distance of 32.6 Å corresponds to a local minimum of these oscillations, the calculated global minimum occurs at around 25 Å. This shows that the indirect interaction between the glutamic-acid molecules cannot completely explained in terms of electronic interactions [26].

Therefore, in the second step we include the effects of structural relaxation. If the structural degrees of freedom

 

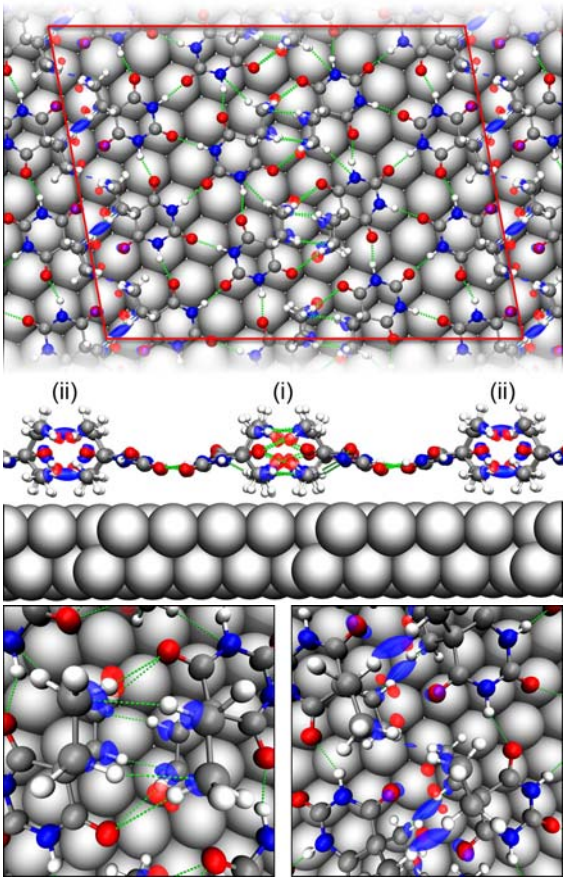


**Figure 3** (color online) Chain structure of the DEB molecule with charge accumulation (blue) and depletion (red) due to the interaction between the chains (Iso-surface value: $0.008e/\text{Å}^3$). The surface periodicity is marked in red and the different inter-chain regions are indicated with (i) and (ii). Below, the dihydrogen bonding region of the above chain structure is shown in detail.

of both adsorbate and substrate are completely relaxed, one obtains a $E_{ads}(x)$ curve that is characterized by very similar minima positions. The global minimum, however, now occurs at about 33 Å. Due to the structural relaxation there are strong modifications of the positions of substrate atoms near to the molecular bonding atoms. By taking the difference of these two energy curves, one can extract the overlapping strain interaction visualized in the upper panel of Fig. 1. Excluding the lowest peak-to-peak distance which indeed includes direct molecular interactions, results in a distance dependence of $E \sim d^{-3}$ for larger separations. This decay behavior fits the elastic-interaction contribution from Lau and Kohn [28] and is connected to the distortion of the substrate lattice caused by the adsorption process.

Next, we turn to the DEB system, for which experimentally observed STM images [12] show highly ordered rows as well. Starting from these observations, our adsorption model for the DEB chains contains twelve molecules within a $\left(\begin{smallmatrix}4 & 4\\ 2 & 8\end{smallmatrix}\right)$ periodicity. The structurally relaxed low-energy structure of the model together with the surface unit cell is shown in Fig. 3 as top and side views. A complex network of hydrogen bonding evolves between the molecules (depicted with green dotted lines in Fig.3). In the following, we call two DEB molecules H-bonded with the CYA like rings together a chain, while the inter-chain region is defined by the alkyl-groups of the molecules (For details see Ref. [10]). In neighboring chains, the molecular sidechains face each other. As can be expected, the intra-chain interactions are mediated by N-H$\cdots$O bonds. But what accounts for the inter-chain interactions, which can be seen in Fig.3? The charge-density difference between the total system and the two separated chains reveals a complex inter-chain interaction. Two different borders exist between each chain and its neighbor chain: (i) the alkyl-side chains are nearly parallel and face each other, thus providing four C-H$\cdots$C and two C-H$\cdots$O bonds with a recognizable polarization, and (ii) the alkyl-side chains are also parallel but shifted along the chain direction, such that they do not face each other in neighboring chains. In the latter case, more C-H$\cdots$H-C "bonds" can be observed with an electron accumulation between the protons. These nearly symmetric "dihydrogen bonds" are vastly dominated by vdW-type interactions [29,30]. In order to assess the strength of this interaction, we performed test calculations for a series of small alkanes. In the simple case of two $C_2H_6$ molecules, for example, the inclusion of vdW interactions results in an attractive force and an energy minimum with a similar electron accumulation between the protons as found above. The ab initio calculation without including vdW-terms yields $E_{WW}^{GGA} = 0.06$ eV, while the inclusion of vdW-interactions results in $E_{WW}^{GGA+vdW} = -0.22$ eV. This agrees well with the values obtained for similar systems in Ref. [30].

**Table 2** Adsorption, binding, interaction and deformation energies per molecule in eV for DEB with and without vdW interactions.

| | $E_{ad}$ | $E_{bond}$ | $E_{ww,intra}$ | $E_{ww,inter}$ | $E_{def}$ |
|---|---|---|---|---|---|
| +vdW | -2.14 | -0.64 | -0.93 | -0.66 | 0.10 |
| -vdW | 0.08 | 0.04 | -0.36 | 0.25 | 0.15 |

The calculated adsorption energy for the DEB chains amounts to -2.14 eV per molecule, thus being three times larger than for the single molecule adsorption of -0.71 eV. Resolving the adsorption energy into its components helps to understand the origin of this large increase: the binding energy that results from the pure chemical interaction with the surface, the inter- and the intra-chain interaction energies and the deformation energy needed to distort the molecules from their gas phase geometry to their geometry in the adstructure. Table 2 summarizes these components. The binding energy accounts for 30%, the intra-chain 44% and the inter-chain interaction 30% of the total adsorp-

tion energy, thus indicating a stronger interaction between the molecules inside of the chains. Apparently, the binding energy to the surface decreases compared to the single molecule adsorption (0.71 eV) while the interaction energy reflects the largest contribution, and no strong deformation is needed to reach the favorable adsorption geometry.

For a direct comparison to the experiment, we calculated constant current STM images (Fig. 2). As illustrated by the overlayed images in part (1) of Fig. 2, the calculated and the experimental STM images agree very well for the DEB chain structure. Furthermore, this comparison shows that the characteristic bright spots are caused by the side chains of the DEB molecules. The brighter areas in the experimental image, thus, represent the inter-chain region (following our definition of a chain above), while there is a dark line in the experimental image along the center of the chains.

Finally, we want to stress again the importance of including dispersive interactions. In Table 2, the respective values for the various components of the adsorption energies are given with and without dispersion interactions. In the latter case, binding and interaction energies decrease essentially, the molecule–surface interaction vanishes nearly completely. The main contribution to the adsorption energies stems from the H-bonds within the chains, while the inter-chain interaction turns to be a destabilizing factor.

While the inter-row distances in the glutamic acid system is caused by indirect electronic and elastic interactions, the DEB system forms highly ordered rows due to vdW interactions between each molecular row. On the one hand, this can be explained by the different adsorption scenarios: glutamic acid adsorbs with covalent bonds to the silver substrate allowing in principle the existence of indirect interactions due to the charge transfer between substrate and adsorbate in contrast to the weak vdW bonding in the case of the DEB molecule where no charge transfer occurs. On the other hand, the chemical structure at the border of the rows determined by the functional groups of the involved molecules differs for the two systems: while glutamic acid faces to the neighboring row with its negative deprotonated carboxyl group leading to a repulsive interaction, the DEB molecule allows with its alkyl side chains a vdW driven attractive interaction. Thus, the row separation of DEB is much smaller than in the case of glutamic acid. Summarizing, the calculations presented here illustrate two effects: on the one hand, the progress of DFT in explaining and reproducing molecular adsorption phenomena, on the other hand, the complexity of the driving forces that come together to determine the final adsorption structure.

The calculations were done using grants of computer time from the Paderborn Center for Parallel Computing ($PC^2$) and the Höchstleistungs-Rechenzentrum Stuttgart. The Deutsche Forschungsgemeinschaft is acknowledged for financial support.

## References

[1] J. V. Barth, Annu. Rev. Phys. Chem. **58**, 375 (2007).
[2] Q. Chen and N. V. Richardson, Nature Mater. **2**, 324 (2003).
[3] A. Hauschild, K. Karki, B. C. C. Cowie, M. Rohlfing, F. S. Tautz, and M. Sokolowski, Phys. Rev. Lett. **94**, 036106 (2005).
[4] W. G. Schmidt, K. Seino, M. Preuss, A. Hermann, F. Ortmann, and F. Bechstedt, Appl. Phys. A **85**, 387 (2006).
[5] A. Ferretti, C. Baldacchini, A. Calzolari, R. D. Felice, A. Ruini, E. Molinari, and M. G. Betti, Phys. Rev. Lett. **99**, 046802 (2007).
[6] M. Nyberg, M. Odelius, A. Nilsson, and L. G. M. Pettersson, J. Chem. Phys. **119**, 12577 (2003).
[7] S. Blankenburg and W. G. Schmidt, Nanotechnology **18**, 424030 (2007).
[8] S. Blankenburg and W. G. Schmidt, Phys. Rev. B **78**, 233411 (2008).
[9] S. Blankenburg and W. G. Schmidt, J. Phys. CM **21**, 185001 (2009).
[10] S. Blankenburg, E. Rauls, and W. G. Schmidt, J. Phys. Chem., in press (2009).
[11] L. J. Prins, F. D. Jong, P. Timmerman, and D. N. Reinhoudt, Nature **408**, 181 (2000).
[12] W. Xu, M. Dong, H. Gersen, E. Rauls, S. Vzquez-Campos, M. Crego-Calama, D. N. Reinhoudt, E. Loegsgaard, I. Sensgaard, T. R. Linderoth, and F. Besenbacher, Small **4**, 1620 (2008).
[13] G. Kresse and J. Furthmller, Comput. Mater. Sci. **6**, 15 (1996).
[14] J. P. Perdew, J. A. Chevary, S. H. Vosko, K. A. Jackson, M. R. Pederson, and D. J. S. C. Fiolhais, Phys. Rev. B **46**, 6671 (1992).
[15] G. Kresse and D. Joubert, Phys. Rev. B **59**, 1758 (1999).
[16] F. Ortmann, W. G. Schmidt, and F. Bechstedt, Phys. Rev. Lett. **95**, 186101 (2005).
[17] F. Ortmann, W. G. Schmidt, and F. Bechstedt, Phys. Rev. B **73**, 205101 (2006).
[18] E. Rauls, S. Blankenburg, and W. G. Schmidt, Surf. Sci. **602**, 2170 (2008).
[19] E. Rauls and W. G. Schmidt, J. Phys. Chem. C **112**, 11490 (2008).
[20] T. E. Jones and C. J. Baddeley, Langmuir **21**, 9468 (2005).
[21] J. Tersoff and D. R. Hamann, Phys. Rev. B **31**, 805 (1985).
[22] W. A. Hofer, Surf. Sci. **71**, 147 (2003).
[23] W. G. Schmidt, F. Bechstedt, and G. P. Srivastava, Phys. Rev. B **52**, 2001 (1995).
[24] V. Humblot, S. Haq, C. Muryn, W. A. Hofer, and R. Ravel, J. Am. Chem. Soc. **124**, 503 (2002).
[25] J. Friedel, Nuovo Cimento Suppl. **7**, 284 (1958).
[26] K. H. Lau and W. Kohn, Suf. Sci. **75**, 69 (1978).
[27] P. T. Sprunger, L. Petersen, E. W. Plummer, E. Laegsgaard, and F. Besenbacher, Science **275**, 1764 (1997).
[28] K. H. Lau, Solid State Commun. **28**, 757 (1978).
[29] C. F. Matta, J. Hernndez-Trujillo, T. H. Tang, and R. F. W. Bader, Chem. Eur. J. **9**, 1940 (2003).
[30] K. N. Robertson, O. Knop, and T. S. Cameron, Can. J. Chem. **81**, 727 (2003).

 